POLITECNICO DI TORINO
Repository ISTITUZIONALE

Automated Estimation of Patient-Specific Boundary Conditions for Cardiovascular Simulations: an Optimal Control Approach

Original
Automated Estimation of Patient-Specific Boundary Conditions for Cardiovascular Simulations: an Optimal Control Approach / Fevola, E., Ballarin, F., Jimenez-Jua, L., Triverio, P., GRIVET TALOCIA, S., Rozza, G.. - ELETTRONICO. - SB3C2021-006:(2021). (2021 Summer Biomechanics, Bioengineering, & Biotransport Conference Virtual Conference June 14 – 18, 2021).

Availability:
This version is available at: 11583/2920612 since: 2021-09-02T15:23:42Z

Publisher:
SB3C Foundation, Inc.

Published
DOI:

Terms of use:

This article is made available under terms and conditions as specified in the corresponding bibliographic description in the repository

Publisher copyright

(Article begins on next page)

09 November 2026

AUTOMATED ESTIMATION OF PATIENT-SPECIFIC BOUNDARY CONDITIONS FOR CARDIOVASCULAR SIMULATIONS: AN OPTIMAL CONTROL APPROACH

Elisa Fevola (1), Francesco Ballarin (2), Laura Jimenez-Juan (3), Piero Triverio (4), Stefano Grivet-Talocia (1), Gianlugi Rozza (2)

(1) Department of Electronics and Telecommunications
Politecnico di Torino
Torino, Italy

(2) mathLab, Mathematics area
SISSA – International School for Advanced Studies
Trieste, Italy

(3) St Michael's Hospital and Sunnybrook Research Institute
University of Toronto
Toronto, Canada

(4) Department of Electrical & Computer Engineering, Institute of Biomaterials & Biomedical Engineering
University of Toronto
Toronto, Canada

INTRODUCTION

In recent years, large advancements have been made in the development of patient-specific cardiovascular models for blood flow simulations. In these simulations, the choice of appropriate boundary conditions is a crucial step, since they have a large influence on the resulting flow rates and hemodynamic parameters of clinical relevance, such as wall shear stress (WSS). In-vivo measurements, if available, can be used to guide the selection of boundary conditions, such that simulation results better match clinical data. A common approach is to split a given inlet flow rate among all outlets according to their area by means of Murray's law [1]. From the obtained flows and an estimate of pressure, the resistance to be placed at each outlet is obtained. However, manual tuning is required to match in-vivo data, which is time consuming and operator dependent. More systematic methods have been proposed based on optimal control [2], Bayesian estimation [3], and Kalman filtering [4].

With optimal control, a rigorous Lagrangian approach [5] is used to determine the optimal value of resistance boundary conditions that match the given in-vivo measurements. Optimal control was applied to a glass replica of cardiovascular models [6] and to coronary artery bypass grafts [2], but using less realistic Neumann-type boundary conditions. In this work, we propose an optimal control framework for determining resistance-type boundary conditions in patient-specific aortic models, starting from flow measurements obtained with 4D-Flow MRI. We show the validity of the proposed framework on a real clinical case, and investigate the influence of the obtained boundary conditions on WSS and oscillatory shear index (OSI).

METHODS

We present the proposed method by considering the aortic arch represented in Fig. 1, with the goal of determining the values of the resistance R_i imposed at each outlet. The anatomy of the vessels was derived from the computed tomography (CT) images acquired with a 320 multidetector scanner (Aquilion ONE, Canon Medical Systems). From the CT images, the vessels surface was reconstructed using SimVascular (www.simvascular.org). A computational mesh was generated with Tetgen. After CT imaging, blood velocity was acquired in-vivo with 4D-Flow magnetic resonance imaging (MRI) with a 3T MRI scanner (MAGNETOM Aera, Siemens Healthineers).
Blood flow in the vessels is modelled with the steady Stokes equations

$$\begin{cases} -\eta\Delta v + \nabla p = f\,, & in\ \Omega \\ \nabla \cdot v = 0, & in\ \Omega \end{cases} \tag{1}$$

At the ascending aorta inlet Γ_{in}, a Poiseuille flow was imposed, whose average value was extracted from the 4D-Flow MRI data of the patient.

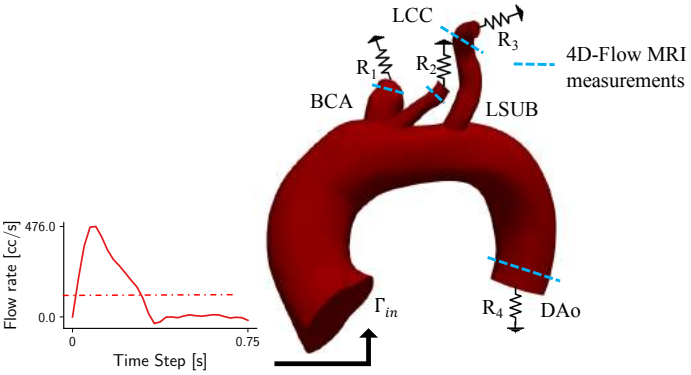

Figure 1: General setting of the proposed framework on a patient's aortic arch.

A no-slip condition was imposed at the vessel walls, assumed to be rigid. At the four outlets, corresponding to descending aorta (DAo), brachiocephalic artery (BCA), left common carotid artery (LCC) and left subclavian artery (LSUB), a resistive-type boundary condition was imposed following the coupled multidomain method proposed in [7]. The unknown resistance values R_i were then determined solving an optimal control problem. Optimal control estimates unknown parameters by minimizing a cost functional constrained by the governing equations of the system.

We defined a cost functional J with the following form:

$$J = \alpha_p \frac{\int_\Omega ||p - p_d||^2 d\Omega}{2\int_\Omega ||p_d||^2 d\Omega} + \sum_{i=1}^{4} \alpha_i \frac{\int_{\Gamma_i} ||v - v_i||^2 d\Gamma_i}{2\int_{\Gamma_i} ||v_i||^2 d\Gamma_i} + \\ + \sum_{i=1}^{4} \beta_i \frac{\int_{\Gamma_i} ||R_i||^2 d\Gamma_i}{2\int_{\Gamma_i} ||R_{i,M}||^2 d\Gamma_i} \quad (2)$$

where α_p is set to 100, α_i and β_i to 1, and $R_{i,M}$ is the resistance value at the outlet Γ_i obtained with Murray's law. The first term in (2) represents the difference between the pressure p obtained from (1) and the patient's average aortic pressure p_d derived from clinical data. The second term relates to the difference between the velocity v from (1) and the average velocity v_i measured at each outlet Γ_i. The third term consists of the norm of the control variables R_i, and acts as a regularization term. For solving the optimal control problem, we adopted an adjoint-based Lagrangian approach [5], first deriving the optimality system containing the first-order optimality conditions, and then recasting it to saddle-point form to obtain a monolithic algebraic system for easier computations. The obtained system was then solved with the open-source libraries FEniCS [8] and multiphenics [9].

RESULTS

The results obtained for the case of Fig. 1 are detailed in Table 1. On the first row, Table 1 reports the patient's average pressure measured non-invasively after MRI, and flow rates measured in-vivo with 4D flow MRI. The second and third row of the table report the values obtained with the boundary conditions estimated with Murray's law and with the proposed method. The pressure and flow values obtained with optimal control match the patient measurements quite closely, indicating a proper assimilation of in-vivo information. While a perfect match would be ideal, this is often not possible in practice, due to the noise and uncertainty affecting in-vivo measurements, and due to the assumptions of the adopted mathematical model (1). By minimizing (2), the proposed approach finds the set of boundary conditions that comes as close as possible to the given in-vivo information.

We also observe that the solution from the proposed method is not too far from the one obtained with Murray's law, where boundary conditions are set on the basis of purely anatomical information [1]. This observation further confirms the physiological validity of the boundary conditions selected by the proposed method. Table 2 reports the resistance values obtained with the two methods, Murray's law and optimal control. The values are similar, except for the LSUB resistance, which differs substantially (23%). To investigate how this difference may affect clinically-relevant hemodynamic parameters, we used the two sets of boundary conditions reported in Table 2 to run two unsteady high-fidelity Navier-Stokes simulations, using SimVascular. Resistance values were used to set three-element Windkessel models at each outlet, assuming a total capacitance of 0.001 cm^5/dyne, distributed among the various outlets with an area-based criterion. Fig. 2 depicts the absolute difference between the OSI computed with the two sets of boundary conditions. While the difference is negligible for the most part of the geometry, the difference reaches 40% of the OSI range (0÷0.5) in the region past the left subclavian artery.

Table 1: Comparison of average aortic pressure and outlet flow rates obtained with Murray's law and with the proposed method.

	Pressure (mmHg)	Flow rates (cm^3/s)			
		BCA	LCC	LSUB	DAo
Patient measurements	98.7	15.9	5.98	8.48	73.1
Murray's law	98.8	19.2	6.19	7.48	86.2
Proposed	95.2	19.8	6.10	9.41	83.9

Table 2: Resistance values obtained with Murray's law and with the proposed method (all values in dyn·s·cm^{-5}).

	DAo	BCA	LCC	LSUB
Murray's law	1,526	6,837	21,241	17,591
Proposed	1,513	6,409	20,801	13,467

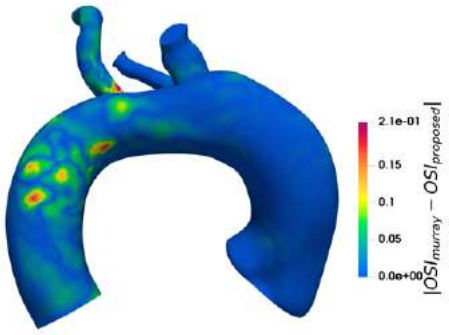

Figure 2: Absolute difference of OSI between Murray's law and the proposed method (back view of the aorta).

DISCUSSION

We proposed a computational framework for the determination of resistance-type outlet boundary conditions based on the assimilation of 4D-Flow MRI measurements by means of optimal control. Our study documents the application of such framework to a real clinical case and shows the influence that the choice of outlet boundary conditions has on OSI, one of the hemodynamic quantities of potential clinical interest. The presence of regions with a considerable difference from Murray's law-based results confirms the crucial role of boundary conditions in hemodynamic modeling, and suggests the need for further research on determining appropriate boundary conditions for computational hemodynamics.

REFERENCES

[1] Murray C.D, *Proc. of the Ntl Acad of Sciences USA*, 1926, 12.3: 207.
[2] Zainib. Z. et al., *Int J for Num Methods in Bio Eng,* 2020, e3367.
[3] Schiavazzi DE et al, *Int J for Num Methods in Bio Eng,* 2017; 33(3): e02799.
[4] Arthurs CJ et al, *Adv Mod Sim Eng Sciences,* 2020; 7(1): 1-37.
[5] Gunzburger MD, *Perspectives in Flow Control and Optimization,* SIAM, 2003.
[6] Koltukluoglu T. S. et al., *J Fluid Mech.,* 2018; 847: 329-364.
[7] Vignon-Clementel IE. et al., *Computer methods in applied mechanics and engineering,* 2006; 195(29-32): 3776-3796.
[8] Alnaes MS. et al., *Arch Numer Softw.,* 2015; 3(100): 9-23.
[9] https://mathlab.sissa.it/multiphenics. 2019